



 Cite this: *RSC Adv.*, 2020, 10, 25629

A naringenin-based benzoxazine with an intramolecular hydrogen bond as both a thermal latent polymerization additive and property modifier for epoxy resins†

 Boran Hao, Rui Yang and Kan Zhang *

Epoxy resins are constantly attracting attention from industrial applications due to their excellent comprehensive properties. However, the traditional curing agents for liquid epoxy resins react with epoxides even at room temperature, which causes difficulties in processing since such mixtures cannot be directly used as single-component materials. In order to improve the shelf life of the mixtures, we have designed an intramolecular hydrogen bond-containing benzoxazine monomer as a smart thermal latent polymerization agent for epoxy resins. The newly obtained benzoxazine, **NAR-a**, has been synthesized from the Mannich condensation of naringenin, aniline and paraformaldehyde. In addition to playing the role of a curing agent, **NAR-a** has also performed as an excellent property modifier for epoxy thermosetting systems. The resulting thermoset based on the **NAR-a**/epoxy thermosetting system exhibits high thermal stability and good intrinsic flame retardance, with a T_g temperature of 201 °C, a T_{d5} temperature of 349 °C, a low CET value (32.4 ppm per °C) and low heat release capacity (HRC of 159.1 J g⁻¹ K⁻¹). The combined long-term storage stability and versatility of the intramolecular hydrogen bond-containing benzoxazine/epoxy system provide a new strategy for the development of one-component epoxy-related thermosetting resins for application in high-performance areas.

 Received 22nd May 2020
Accepted 22nd June 2020

DOI: 10.1039/d0ra04702c

rsc.li/rsc-advances

Introduction

Epoxy resins are very important thermosetting polymers that are widely applied in various industries.^{1–3} Though many curing agents such as amines,^{4,5} imidazoles⁶ and phenols⁷ have attracted particular attention due to their very high reactivity with epoxides, the polymerization of a liquid epoxy resin containing the above curing agents occurs gradually even at room temperature. Such a shortcoming makes it difficult to use epoxy resins as single-component products for application in industries. In order to improve the storage stability, some latent polymerization additives have been developed.^{8,9} Interestingly, the manipulation of intramolecular hydrogen bonding in the structure of curing agents can significantly enhance the shelf life of epoxy resins.¹⁰

Polybenzoxazine is a relatively new type of cross-linked polymer, which has been drawing particularly strong interest from both academic researchers and industrial engineers due to its excellent features, such as near-zero shrinkage during curing,^{11,12} high thermal stability,^{13–15} low- k (dielectric constant)

values,^{16,17} low surface free energy¹⁸ and flexible macromolecular design capability.^{19,20} Besides, polybenzoxazine can be directly prepared by the thermally activated ring-opening polymerization of 1,3-benzoxazine.^{21,22} Because the polymerization of benzoxazine generates phenolic groups, the copolymerization between benzoxazine and epoxy is anticipated since it is well-known that the phenolic $-OH$ groups can react with epoxides at elevated temperatures.^{7,23} Ishida and co-workers reported that the copolymerization of **BA-a** (a benzoxazine monomer derived from bisphenol-A, aniline and formaldehyde) and epoxy resulted in thermosets that possess a higher cross-linking density and T_g temperatures than **BA-a**-based polybenzoxazine.²³ On the other hand, the relatively stable oxazine ring in benzoxazines benefits the long shelf life of benzoxazine/epoxy thermosetting systems. However, the polymerization of epoxy/benzoxazine resin systems requires much higher polymerization temperatures than epoxy resins with traditional curing agents since the copolymerization can only take place after the ring-opening of the oxazine ring. Therefore, exploring new benzoxazines with low polymerization temperature is crucial for meeting the requirements for the development of high-performance epoxy/benzoxazine thermosetting systems.

Recently, a few benzoxazines containing built-in latent catalytic functionality have been developed,^{17,24,25} in which the intramolecular hydrogen bonding supports the latent form,

School of Materials Science and Engineering, Jiangsu University, Zhenjiang 212013, China. E-mail: zhangkan@ujs.edu.cn

† Electronic supplementary information (ESI) available. See DOI: 10.1039/d0ra04702c



which can still be broken upon heating to form a very reactive phenolic $-OH$ that can activate the curing process at much lower temperatures than usual. Since these benzoxazines bear unreacted phenolic $-OH$ groups, they are expected to react with epoxy resins in advance of the ring-opening polymerization of oxazine rings. Surprisingly, using such a smart method for developing benzoxazine/epoxy thermosetting systems has not been previously reported.

In this work, a bis-benzoxazine monomer (**NAR-a**) based on naringenin, aniline and paraformaldehyde has been synthesized.

This newly obtained benzoxazine was blended with epoxy resins behaving as both an efficient initiator and a powerful property modifier. In addition, the built-in intramolecular hydrogen bond in the structure of **NAR-a** exhibited good stability, thus being the latent form of the thermosetting resin, enhancing both its shelf life and that of the **NAR-a**/epoxy thermosetting systems. As soon as the intramolecular hydrogen bond in **NAR-a** is broken upon heating, the phenolic $-OH$ becomes more acidic, and can react with epoxides and catalyze the oxazine ring polymerization at much lower temperatures. Herein, the molecular design of the naringenin-based benzoxazine monomer and the hydrogen bonding interaction are investigated. The thermal properties of the corresponding thermosets based on **NAR-a**/epoxy resin systems are also evaluated. **NAR-a** is both a latent polymerization additive and a property modifier for epoxy resins. All results obtained in this study indicate an extremely simple but highly powerful synthetic approach for the design of latent catalyst-containing benzoxazine/epoxy thermosetting systems for application in many chemical industries.

Experimental

Materials

Naringenin (98%) and 4,4'-diaminodiphenylmethane (**DDM**) were purchased from Energy Reagent, China, and used as received. Aniline (98%), paraformaldehyde (97%), hexane, ethyl acetate and toluene were obtained from Aladdin Reagent, China. The epoxy resin, diglycidyl ether of bisphenol A (**DGEBA**), having an epoxy equivalent weight of 185 g eq.⁻¹, was kindly supported by Coryes Co. Ltd, China. A bisphenol-A and aniline based benzoxazine monomer, namely **BA-a**, was prepared according to the previously reported procedure.²⁰

Characterization

NMR spectra of the benzoxazine monomer in $CDCl_3$ and $DMSO-d_6$ were recorded on a Bruker AVANCE II (400 MHz) spectrometer. Elemental analysis was performed using an Elementar Vario EL-III analyzer. A Fourier transform infrared (FT-IR) spectrophotometer (Nicolet Nexus 670) was used to obtain FT-IR spectra of samples with 32 scans in the wave-number range of 400–4000 cm^{-1} . High-resolution mass spectrometry (HR-MS) was carried out on a mass spectrometer (Bruker solanX 70 FT-MS). Differential scanning calorimetry (DSC) curves of the benzoxazine monomer and different epoxy-

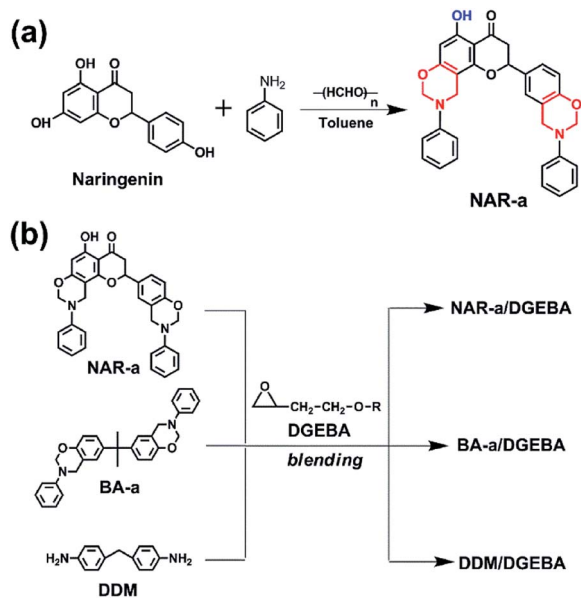
related thermosetting resins were recorded on a DSC apparatus (TA 2920). The heating rate of all DSC measurements was set at 10 $^{\circ}C\ min^{-1}$ and the testing was conducted under a nitrogen atmosphere. Thermogravimetric analysis (TGA) was performed on a TGA apparatus (TA Q500). The heating rate of the TGA analysis was set at 10 $^{\circ}C\ min^{-1}$ in N_2 from room temperature to 800 $^{\circ}C$. Thermal mechanical analysis (TMA) was conducted on a NETZSCH TMA/402F4 instrument at a heating rate of 5 $^{\circ}C\ min^{-1}$. Dynamic mechanical analysis (DMA) of thermoset samples was carried out with a NETZSCH DMA/242E analyzer at a heating rate of 3 $^{\circ}C\ min^{-1}$. The DMA tests were performed using tension mode with an amplitude of 10 μm and a frequency of 1 Hz. The fire-related properties of thermosets were evaluated by a microscale combustion calorimeter (MCC, Fire Testing Technology). The heat release capacity (HRC, $J\ g^{-1}\ K^{-1}$) and the total heat release (THR, $kJ\ g^{-1}$) values were obtained using this MCC calorimeter. The measurements for all thermosets were performed from 100 to 750 $^{\circ}C$ at a heating rate of 1 $K\ s^{-1}$. An 80 $mL\ min^{-1}$ stream of N_2 with thermal decomposition products were mixed with a 20 $mL\ min^{-1}$ stream of O_2 , and all the above mixtures were placed in the combustion furnace at a constant temperature of 900 $^{\circ}C$.

Synthesis of 5-hydroxy-9-phenyl-2-(3-phenyl-3,4-dihydro-2H-benzo[e][1,3]oxazin-6-yl)-2,3,9,10 tetrahydrochromeno[8,7-e][1,3]oxazin-4(8H)-one (abbreviated as **NAR-a**)

Paraformaldehyde (1.50 g, 0.05 mmol), naringenin (2.72 g, 0.01 mol) and 50 mL of toluene were mixed into a 250 mL single-neck flask with a condenser under magnetic stirring. The reaction was conducted at room temperature for 10 min, and then aniline (1.86 g, 0.02 mmol) was slowly added to this system. The reaction mixtures were warmed to 100 $^{\circ}C$ and stirred at this temperature for 4 h. After the reaction, the chemical mixtures were cooled to room temperature and washed 3 times using deionized water. The crude product was collected by removing the solvent using a rotary evaporator. The crude sample was further purified by recrystallization from a solvent mixture of hexane and ethyl acetate in a 3 : 1 ratio. Finally, white needle-like crystals were obtained (yield *ca.* 76%). ¹H NMR (400 MHz, $CDCl_3$), ppm: δ = 12.31 (s, 1H, OH), 7.32–6.83 (13H, Ar), 5.98 (s, 1H, Ar), 5.40 (d, 4H, O-CH₂-N, oxazine ring), 5.28 (dd, 1H, O-CH-CH₂-), 4.67–4.57 (d, 4H, Ar-CH₂-N, oxazine ring), 3.06–2.73 (m, 2H, -CH-CH₂-C=O). FT-IR spectra (KBr), cm^{-1} : 1644 (C=O stretching), 1238 (C-O-C antisymmetric stretching), 926 (benzoxazine related band). Elemental analysis: calculated for $C_{31}H_{26}N_2O_5$: C, 73.50; H, 5.17; N, 5.53. Found: C, 73.41; H, 5.20; N, 5.51. HRMS-ESI (m/z): $[M + H]^+$ calculated for $C_{31}H_{27}N_2O_5^+$, 507.5559; found, 507.1911.

Preparation and polymerization of epoxy-based thermosetting resins

NAR-a, **BA-a** and **DDM** were used as curing agents for **DGEBA**, respectively. The ratio of **DGEBA** to **NAR-a**, **BA-a** and **DDM** was fixed according to the stoichiometry (the molar ratio of the epoxy to N-H, -OH or oxazine ring was 1 : 1). **NAR-a**, **BA-a** and



Scheme 1 (a) Synthesis of naringenin-based benzoxazine (NAR-a). (b) Preparation of epoxy-based thermosetting systems.

DDM were blended with DGEBA by vigorously stirring to form the homogeneous NAR-a/DGEBA, BA-a/DGEBA and DDM/DGEBA, respectively. NAR-a/DGEBA and DDM/DGEBA were polymerized at 120, 140, 160, 180, 200 and 220 °C for 1 h each, yielding poly(NAR-a/DGEBA) and poly(DDM/DGEBA), respectively. BA-a/DGEBA was polymerized stepwise, with each step at 120, 140, 160, 180, 200, 220 and 240 °C, and kept for 1 h at each stage, finally achieving poly(BA-a/DGEBA).

Results and discussion

Synthesis of NAR-a

As shown in Scheme 1, a new benzoxazine monomer, NAR-a, has been synthesized using the raw materials of naringenin,

aniline and paraformaldehyde. In particular, a free phenolic hydroxyl group can persist in NAR-a after the one-pot Mannich reaction. In general, reactions with multiple steps and extra acid catalysts had to be applied to achieve phenolic hydroxyl group-containing benzoxazines since one of the hydroxyl groups should be unreacted.^{26,27} Besides, the reaction temperatures also have to be carefully handled because the phenolic -OH has a catalytic effect on the ring-opening of the oxazine ring, which does not benefit the oxazine ring closure. Based on the existence of the intramolecular hydrogen bond between one of the three phenolic groups in naringenin and its neighbouring carbonyl group, NAR-a with the phenolic hydroxyl functionality was directly obtained according to a general Mannich condensation. The detailed structure of NAR-a was confirmed by combining the results of FT-IR (Fig. S1†), and ¹H, ¹³C and 2D NMR spectroscopies as well as elemental analysis and HR-MS.

Generally, the typical ¹H and ¹³C NMR signals for the methylene pairs in bisbenzoxazine monomers consist of two singlets attributed to the symmetry of the chemical structure.^{19,20} As shown in Fig. 1a, the proton signals assigned to the two O-CH₂-N groups in NAR-a are heavily overlapped at 5.40 ppm. Besides, the resonances due to the two Ar-CH₂-N groups associating with each oxazine ring were found from 4.67 to 4.57 ppm. The integration ratio for the protons of O-CH₂-N and Ar-CH₂-N perfectly correspond to four hydrogen atoms, clearly suggesting that no isomers were formed in NAR-a. This newly obtained benzoxazine possesses an asymmetric chemical structure, resulting in the separated signals of the Ar-CH₂-N group. In addition, the protons related to the methylene and methyne from naringenin appeared at 3.06–2.73 and 5.28 ppm, respectively.

The 2D ¹H-¹H NOESY NMR spectrum of NAR-a was then recorded to further confirm the detailed structure. As seen from Fig. S2,† the proton signal of H_c presented no NOE interaction with other protons, strongly indicating that it was in the *ortho*-position of the unreacted -OH group. Conversely, if H_c was replaced during the oxazine ring formation, there would have

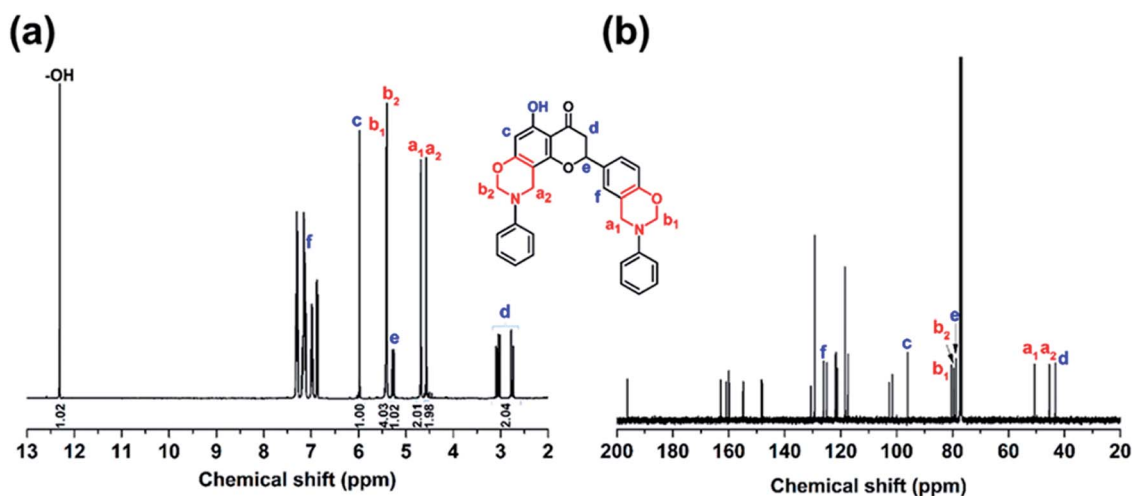


Fig. 1 ¹H (a) and ¹³C (b) NMR spectra of NAR-a using CDCl₃ as the solvent.

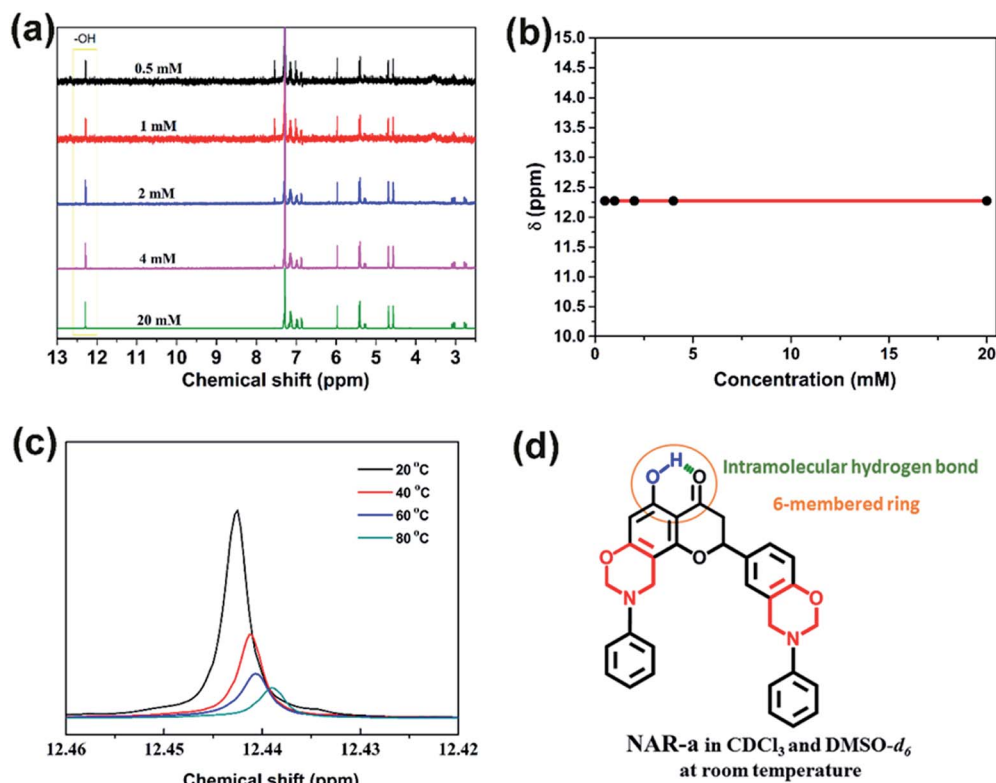


Fig. 2 (a) ^1H NMR spectra of **NAR-a** at different concentrations in CDCl_3 . (b) The results of the concentration-dependence experiments in CDCl_3 for **NAR-a** at different concentrations. (c) Peak shifting of the phenolic proton of **NAR-a** in ^1H NMR spectra using $\text{DMSO}-d_6$ as solvent at 20, 40, 60 and 80 $^\circ\text{C}$. (d) Simplified molecular structures of **NAR-a** possessing a 6-membered intramolecular hydrogen bond.

been a free proton in the *para*-position with respect to the $-\text{OH}$ group, which should be close enough to show the NOE effect with H_e . However, such interaction was not observed in the 2D $^1\text{H}-^1\text{H}$ NOESY NMR spectrum of **NAR-a**. Concerning the NOE effect corresponding to the methylene protons in the oxazine ring, it was observed that H_f exhibited an obvious interaction with H_{a1} , which interacted with H_{b1} . Therefore, the complete ^1H NMR spectral elucidation of **NAR-a** is shown in Fig. 2a. The ^{13}C NMR spectrum of **NAR-a** is depicted in Fig. 2b. The full assignments of carbon resonances were achieved according to the corresponding correlations in the $^1\text{H}-^{13}\text{C}$ HMQC NMR spectrum (Fig. S3 †).

Intramolecular hydrogen bonding study

In order to examine the intramolecular hydrogen bonding in **NAR-a**, we carried out a series of spectroscopic experiments in CDCl_3 and $\text{DMSO}-d_6$. The corresponding results are shown in Fig. 2.

First of all, the existence of the intramolecular hydrogen-bonding system in **NAR-a** was supported by ^1H NMR spectra, using CDCl_3 as solvent. In general, the quality and chemical shifts of the proton signals of $-\text{OH}$ groups are highly influenced by different deuterated solvents. For example, CDCl_3 has the particularity of forming an intermolecular proton-deuterium exchange with $-\text{OH}$ -containing samples, causing some difficulties in analysis due to the signal distortion. Although some

signals can be detected, the corresponding integration is rarely acceptable. However, the signal quality of $-\text{OH}$ could be restored by eliminating the proton-deuterium exchange if the mobility of the hydroxyl group was significantly reduced. As clearly seen from Fig. 1a, a strong singlet with a perfect integration ratio for the $-\text{OH}$ was observed for **NAR-a**, supporting the existence of a very strong hydrogen bonding system of $-\text{OH}$ groups. Secondly, this hydrogen bond was further supported in the same spectrum since this $-\text{OH}$ group exhibited a very high chemical shift at 12.31 ppm. Such unusually high shifting of the hydroxyl group is because stronger hydrogen bonds cause the involved proton to be more deshielded. A concentration-dependence experiment using CDCl_3 as the solvent was further carried out. As shown in Fig. 2a and b, no variation in the chemical shift of the $-\text{OH}$ signal was observed while varying the concentration of the **NAR-a** solutions. As a result, the above NMR analyses strongly indicate the existence of the intramolecular hydrogen-bonding system in **NAR-a**.

We also recorded the ^1H NMR spectrum of **NAR-a** in $\text{DMSO}-d_6$ (Fig. S4 †). Fig. 2c shows that the $-\text{OH}$ signal shifted to higher fields (lower ppm) on increasing the temperature, indicating that the intramolecular hydrogen-bonding system could become weaker upon heating. In addition, there should be a temperature at which the hydrogen bond would be broken and let the proton go free. Thus, the latent-catalyst can be activated by breaking the hydrogen bonding system upon

heating since the ring-opening polymerization of benzoxazine resins is acid-catalyzed. As a result, the intramolecular hydrogen bonding system formed in **NAR-a** in both CDCl_3 and $\text{DMSO-}d_6$ at room temperature can be depicted as shown in Fig. 2d.

Polymerization behaviors of benzoxazine and benzoxazine/epoxy resins

The polymerization process of **NAR-a** was investigated by DSC and *in situ* FT-IR spectroscopy. As shown in Fig. 3, a thermal event exhibited an endothermic peak due to the melting behavior, for which a minimum was observed at 173 °C. An exothermic process was another thermal event, in which the maximum was at 180 °C. This exothermic peak was assigned to the ring-opening polymerization behavior of benzoxazine. However, its corresponding onset was not detected because the polymerization process was activated immediately upon melting. The very low temperature for the polymerization process of **NAR-a** successfully supports our new chemical design of a latent catalyst-containing benzoxazine resin. In addition, Fig. 3 also shows a comparison of the TGA and DSC curves of **NAR-a**. As seen from the TGA curve, ~7.7% of weight loss occurred from 175 °C to 300 °C, which was due to the cleavage of the zwitterionic intermediate, forming very unstable phenolic species and *N*-methylethaniline.^{28,29}

In situ FT-IR analysis was then carried out to further study the polymerization of **NAR-a** (Fig. S5†). The characteristic absorption bands around 1238 cm^{-1} (C–O–C antisymmetric stretching mode) and 926 cm^{-1} (benzoxazine related mode) were used to study the ring-opening polymerization of the oxazine rings belonging to **NAR-a**.^{30,31} As seen in Fig. S5,† both bands showed no obvious changes after the thermal treatment at 140 °C. However, the complete disappearance of characteristic bands after further thermal treatment at 160 °C strongly supported the above DSC results, where it was found that **NAR-a** was polymerized through a thermal latent-catalyst efficiency. The above DSC and FT-IR results indicate the existence of a hydrogen-bonding system that makes **NAR-a** very stable and easy to store at moderate to low temperatures. Fig. S6† shows

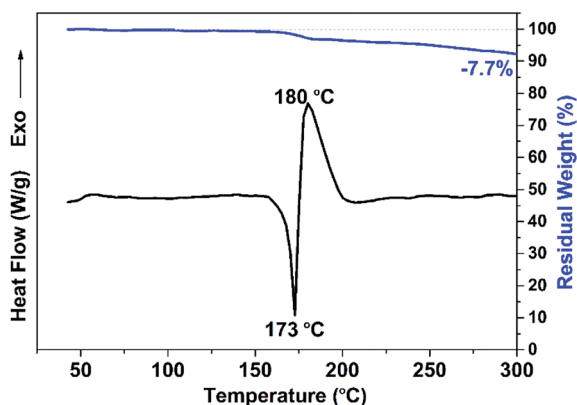


Fig. 3 TGA vs. DSC plots of **NAR-a** (heating rate of 10 °C min^{-1} under a N_2 atmosphere).

the full FT-IR spectra of freshly synthesized **NAR-a** as well as that after three months of storage without any particular protection. As expected, no obvious changes were observed in the corresponding spectra, suggesting the easy storage with demonstrated long shelf-life.

All these advantages are mostly due to the presence of the latent catalyst characteristics in **NAR-a**. We should highlight that these benefits are not only for this monomer in itself, but they can widely be used as thermal latent polymerization additives to enhance other thermosetting systems.

To expand its applications, **NAR-a** should be evaluated as a modifier for the more universal thermosets, such as epoxy resin. To achieve this goal, **NAR-a** was further applied as a curing agent in epoxy thermosetting systems, and a new thermosetting system, **NAR-a/DGEBA**, was prepared in this study. Two counterparts, **BA-a/DGEBA** and **DDM/DGEBA** were also prepared, which were investigated to gain deep insight into the polymerization processes and properties of the **NAR-a/DGEBA** thermosetting system.

The non-isothermal polymerization behaviors of **NAR-a/DGEBA**, **BA-a/DGEBA**, and **DDM/DGEBA** were also monitored by DSC. As seen from Fig. 4a, all systems showed no melting peaks, which could be due to the formation of a eutectoid in the molecular homogeneity after the melt blending of each thermosetting resin. The exothermic peak assigned to the polymerization of the epoxy resin with **BA-a** as a curing additive had

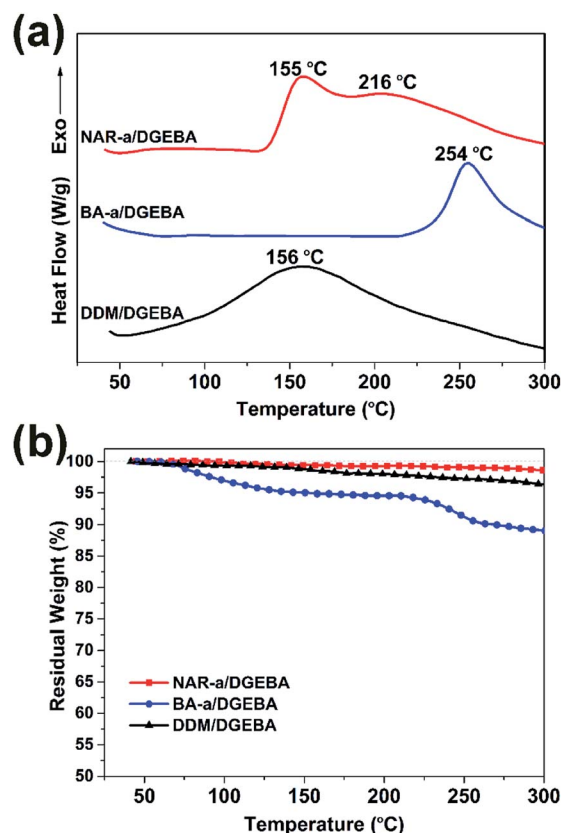


Fig. 4 (a) DSC thermograms of **NAR-a/DGEBA**, **BA-a/DGEBA**, and **DDM/DGEBA**. (b) TGA thermograms of each thermosetting system.

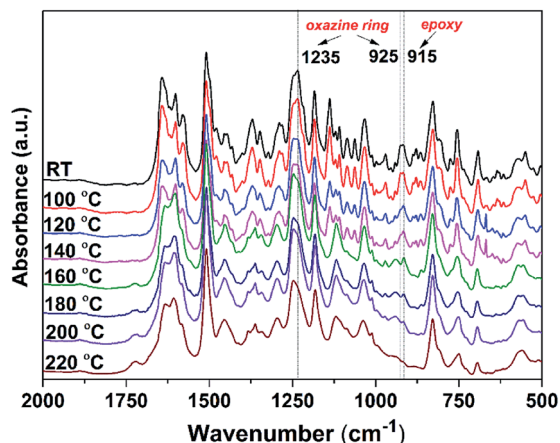
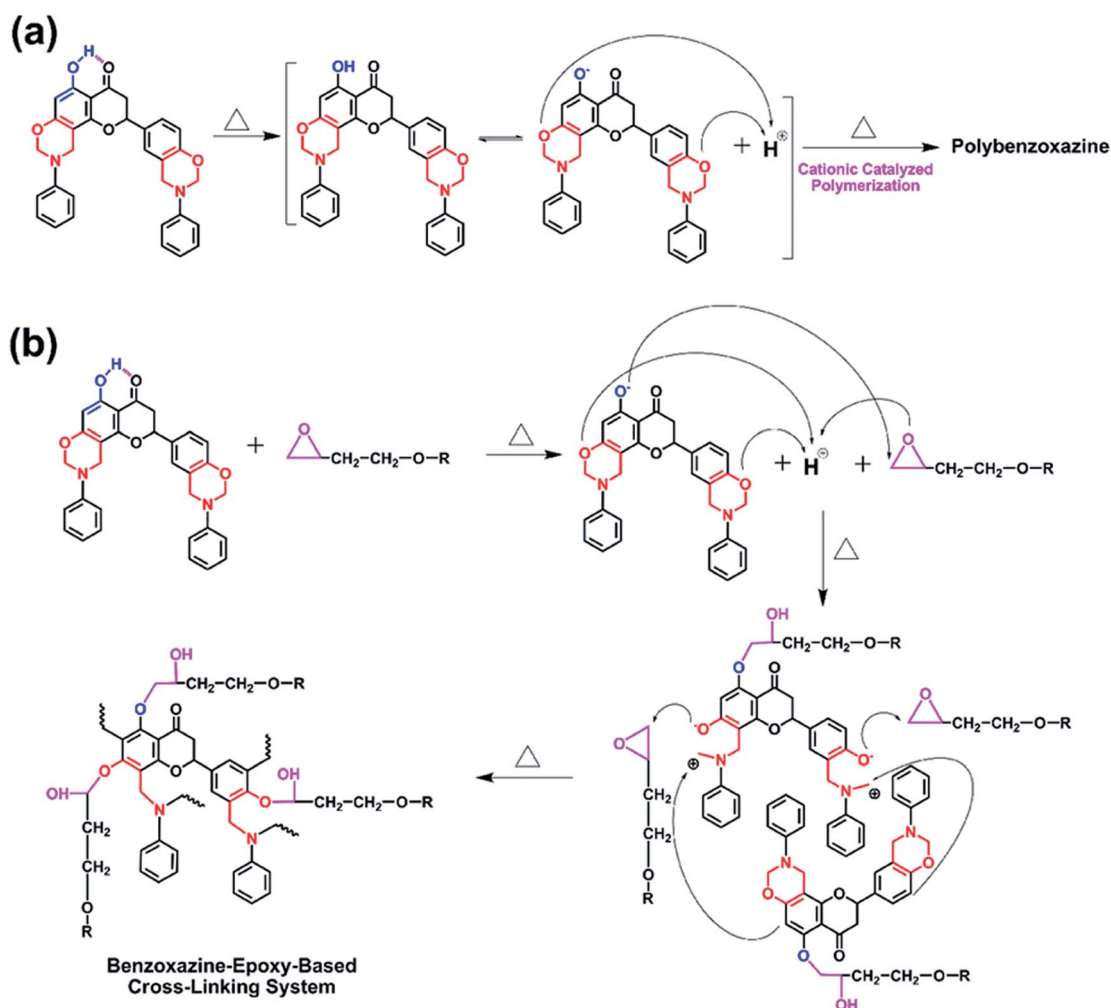


Fig. 5 *In situ* FT-IR spectra of NAR-a/DGEBA during the step-by-step polymerization reaction.

a maximum centered at 254 °C, which was much higher than that of the other two thermosetting systems. Although some phenolic groups generated from impurities in **BA-a** were

expected to react with epoxides at a lower temperature, the copolymerization between benzoxazine and epoxy can only take place after the opening of the oxazine ring, leading to the very high polymerization temperature of **BA-a/DGEBA**. Moreover, **DDM/DGEBA** exhibited a broad exothermic peak with a maximum centered at 156 °C. The primary amine from **DDM** showed very high reactivity in the reaction with epoxides, resulting in a lower polymerization temperature for **DDM/DGEBA**. Here, it should be emphasized that the polymerization of the **DDM/DGEBA** thermosetting system can even proceed gradually at room temperature. Therefore, this makes it difficult to store the **DDM/DGEBA** mixture as a single-component material during the application.

Interestingly, **NAR-a/DGEBA** exhibits polymerization behavior that is different from the other two systems. The exothermic peak attributed to the polymerization of **NAR-a/DGEBA** has two maximums centered at 155 and 216 °C, respectively, indicating the existence of at least two different thermal events during the polymerization. It was mentioned previously that the intramolecular hydrogen bond in **NAR-a** could be weak enough to release the proton at a certain high



Scheme 2 Proposed mechanisms of the built-in latent catalyst activity and polymerization for NAR-a (a) and NAR-a/DGEBA (b).

temperature, so it is reasonable to predict that the exothermic peak with lower temperature can be partially attributed to the reaction between the free phenolic groups and epoxides. Meanwhile, the oxazine ring can also be activated at this stage because the ring-opening polymerization of oxazine is acid-catalyzed. Therefore, it is reasonable that the exothermic peak from the DSC thermogram of **NAR-a/DGEBA** could be attributed to the copolymerization of the generated phenolic -OH in polybenzoxazine with the residual epoxides. No obvious variation was found from the FT-IR spectra of freshly prepared **NAR-a/DGEBA** after three months of storage (Fig. S7†), suggesting that this newly obtained benzoxazine/epoxy thermosetting system also possesses the advantage of a long shelf-life.

The thermal stability of each thermosetting system during the polymerization process was then evaluated by TGA. As shown in Fig. 4b, the traditional epoxy resin system, **DDM/DGEBA**, had ~4% of weight loss after the TGA measurement. **BA-a/DGEBA** showed the initial weight loss starting at ~75 °C and almost ~11% weight loss was observed at 300 °C. Although benzoxazines as curing additives for epoxy resins are well known, the polymerization of epoxy resins with benzoxazine proceeds only after the opening of the oxazine ring. Thus, the low-temperature weight loss of **BA-a/DGEBA** was not unexpected because both components involved in this system only show small molecular weight before the ring-opening polymerization

of **BA-a**. On the contrary, another benzoxazine/epoxy system, **NAR-a/DGEBA**, exhibited the most excellent thermal stability during the polymerization amongst these three thermosetting systems. Therefore, the latent effect and multiple copolymerization behaviors in **NAR-a/DGEBA** significantly enhance its thermal stability at elevated temperatures.

To gain deeper insight into the polymerization processes of the **NAR-a/DGEBA** thermosetting system, *in situ* FT-IR analysis was also performed. As depicted in Fig. 5, the characteristic absorption band related to the epoxy group at 915 cm^{-1} ,³² as well as the oxazine related bands at 1238 cm^{-1} (C–O–C anti-symmetric stretching mode) and 926 cm^{-1} (oxazine-ring related mode), all gradually decreased with the progress of thermal treatments starting from 120 °C. There was a complete disappearance of the characteristic bands of benzoxazine after heating at 160 °C. Moreover, the epoxy absorption in **NAR-a/DGEBA** disappeared completely after the final polymerization step. These variations in FT-IR spectra fully support our hypothesis above for the polymerization behaviors of **NAR-a/DGEBA** based on the DSC thermogram. The free phenolic groups in **NAR-a** can react with epoxides as well as act as an efficient catalyst for the ring-opening polymerization of the oxazine ring in the initial polymerization stage. Afterwards, the newly generated phenolic groups in polybenzoxazine further

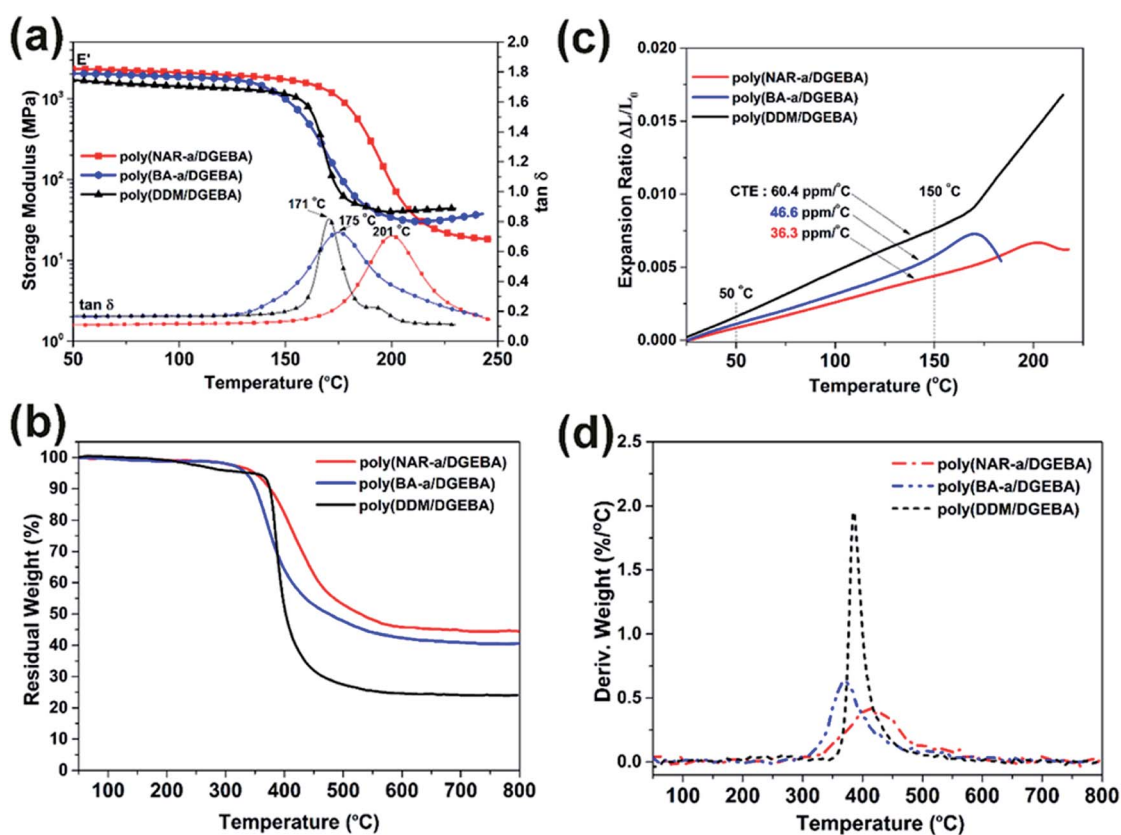


Fig. 6 (a) Dynamic mechanical spectra of poly(**NAR-a/DGEBA**), poly(**BA-a/DGEBA**) and poly(**DDM/DGEBA**). (b) Thermomechanical analysis of thermosets. (c) Thermogravimetric analysis of poly(**NAR-a/DGEBA**), poly(**BA-a/DGEBA**) and poly(**DDM/DGEBA**). (d) DTG curves of epoxy-based thermosets.

crosslinked with the residual epoxides in the **NAR-a/DGEBA** thermosetting system.

Based on the above DSC and FT-IR results, the proposed mechanisms for the polymerization behaviors of **NAR-a** and **NAR-a/DGEBA** thermosetting systems are shown in Scheme 2. Our proposed mechanisms presented in Scheme 2 have taken into consideration the already established acid-catalyzed polymerization of benzoxazine resins.³³

Thermal and fire-related properties of benzoxazine-epoxy-based thermosets

The thermomechanical properties of thermosets based on **NAR-a/DGEBA**, **BA-a/DGEBA** and **DDM/DGEBA** have been evaluated by both DMA and TMA measurements. The T_g values were determined by DMA, and were obtained from the temperature at the peak maximum of the $\tan \delta$ as a function of the temperature. As shown in Fig. 6a, **poly(BA-a/DGEBA)** and **poly(DDM/DGEBA)** had T_g temperatures at 175 and 171 °C, respectively. Besides, **poly(NAR-a/DGEBA)** exhibited the highest T_g temperature at 201 °C. Notably, **poly(NAR-a/DGEBA)** also possessed the highest value of storage modulus among these epoxy-based thermosets in the temperature range of 50–200 °C, indicating the formation of highly cross-linked networks based on our newly developed latent-catalyst-containing benzoxazine/epoxy thermosetting system. TMA was carried out to obtain the coefficient of thermal expansion (CTE) values of the thermosets. As can be seen from Fig. 6b, CTE values for **poly(BA-a/DGEBA)** and **poly(DDM/DGEBA)** obtained from TMA in the temperature range of 25–150 °C were 46.6 and 60.4 ppm per °C, respectively. **Poly(NAR-a/DGEBA)** exhibited a CTE value of 36.3 ppm per °C, which is much lower than the values obtained from **poly(BA-a/DGEBA)** and **poly(DDM/DGEBA)**. As a result, the benzoxazine-modified epoxy resins show much lower CET values as compared with the CET of traditional epoxies.³⁴ Specifically, cross-linked networks of epoxies with units contributed from

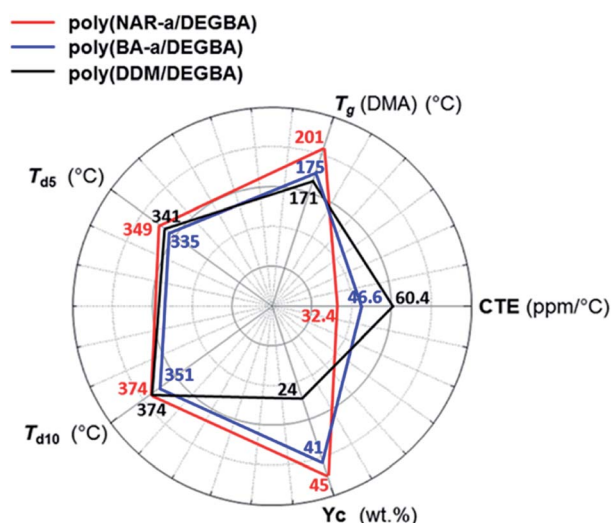


Fig. 7 Comparison of the thermal properties of **poly(NAR-a/DGEBA)**, **poly(BA-a/DGEBA)** and **poly(DDM/DGEBA)**.

our newly developed benzoxazine, **NAR-a**, led to a significantly decreased CET value.

The thermal stabilities of **poly(NAR-a/DGEBA)**, **poly(BA-a/DGEBA)** and **poly(DDM/DGEBA)** were evaluated by TGA under N_2 . As shown in Fig. 6c and d, an obvious weight loss with a very high degradation rate from 350 to 450 °C was observed for **poly(DDM/DGEBA)**. In contrast, **poly(NAR-a/DGEBA)** and **poly(BA-a/DGEBA)** showed a relatively stable degradation rate during their initial weight loss stages. However, **poly(BA-a/DGEBA)** showed the lowest T_{d5} (5% weight loss temperature) of 335 °C, which is due to the degradation of the defect structures originating from its polybenzoxazine networks.³⁵ The copolymerization between benzoxazine and epoxy in **BA-a/DGEBA** mostly took place after the ring-opening of the oxazine ring, indicating that such defect structures still existed in this copolymer system. Besides, **poly(NAR-a/DGEBA)** showed excellent thermal stability with T_{d5} of 349 °C and T_{d10} (10% weight loss temperature) of 374 °C, respectively. The enhanced thermal properties of **poly(NAR-a/DGEBA)** are mainly attributed to the highly cross-linked networks formed from multiple types of copolymerization between **NAR-a** and epoxy resins, as well as

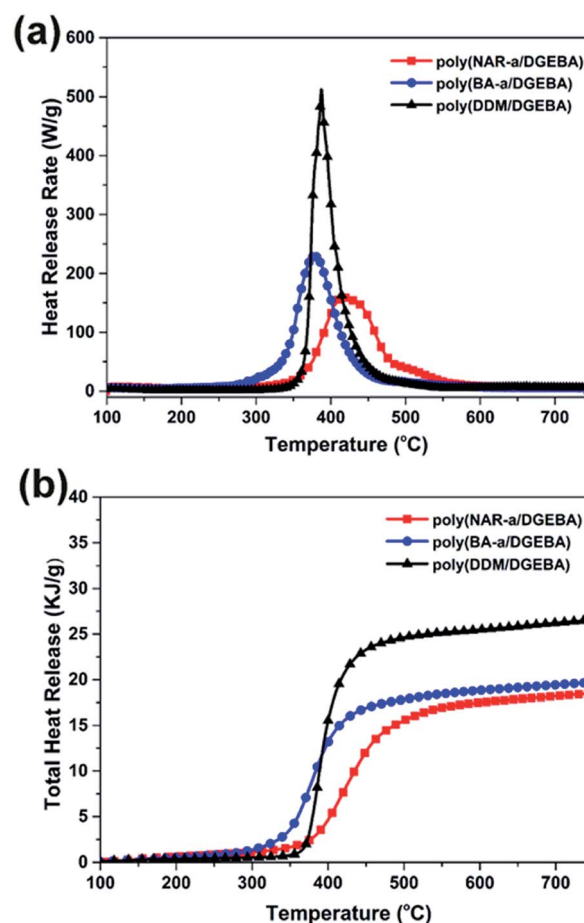


Fig. 8 (a) Heat release rate (HRR) versus temperature for **poly(NAR-a/DGEBA)**, **poly(BA-a/DGEBA)** and **poly(DDM/DGEBA)**. (b) Total heat release (THR) versus temperature for **poly(NAR-a/DGEBA)**, **poly(BA-a/DGEBA)** and **poly(DDM/DGEBA)**.

the existence of the polybenzoxazine segments with intrinsically high thermal stability. Moreover, **poly(NAR-a/DGEBA)** also showed a high Y_c (char yield) value of 45% at 800 °C in nitrogen. The thermal property data of these three epoxy-based thermosets are summarized in Fig. 7, which demonstrate the high thermal stability of **poly(NAR-a/DGEBA)**.

Specifically, the pronounced broadness of the derivative peak of **poly(NAR-a/DGEBA)** (Fig. 6d) exhibited a very slow degradation rate over a wide temperature range, which is considered as an advantage for low flammability.³⁶ Therefore, we looked at the flame-retardant capability of each thermoset by limiting oxygen index (LOI) tests. The LOI parameter can be determined from the Y_c values based on TGA results by using the van Krevelen equation,³⁷ from which the LOI values of **poly(NAR-a/DGEBA)**, **poly(BA-a/DGEBA)** and **poly(DDM/DGEBA)** at 800 °C were found to 35.5, 33.9 and 27.1, respectively. **poly(DDM/DGEBA)** has an LOI value slightly lower than 28, which falls in the slow-burning region ($21 < \text{LOI} < 28$). However, both **poly(NAR-a/DGEBA)** and **poly(BA-a/DGEBA)** possess LOI values greater than 28, which is in the self-extinguishing region,³⁸ indicating that the benzoxazine-modified epoxy resins are excellent candidates for use as flame retardant materials.

Microscale combustion calorimetry (MCC) analysis was finally carried out to investigate the quantitative aspects of the flammability of thermosets.^{39,40} As shown in Fig. 8a, the MCC curves of **poly(NAR-a/DGEBA)**, **poly(BA-a/DGEBA)** and **poly(DDM/DGEBA)** revealed HRC values of 159.1, 229.6, and 512.1 J g⁻¹ K⁻¹, respectively. Besides, **poly(NAR-a/DGEBA)** and **poly(BA-a/DGEBA)** exhibited THR values of 18.5 and 19.7 kJ g⁻¹, while **poly(DDM/DGEBA)** exhibited a much higher THR value of 26.5 kJ g⁻¹ (Fig. 8b). Among these thermosets obtained in this study, **poly(NAR-a/DGEBA)** showed the lowest flammability, supported by its very low HRC and THR values, indicating that the higher degree of cross-linking can enhance the flame retardancy of epoxy-related thermosetting systems. Though the HRC value of **poly(NAR-a/DGEBA)** is higher than many polybenzoxazines with excellent flame retardancy,^{41,42} it is substantially lower than the traditional and some recently reported high-performance epoxy thermosetting systems.⁵ Therefore, the **NAR-a/DGEBA** thermosetting system may have great potential in applications that benefit both high thermal stability and low flammability.

Conclusions

A novel latent catalyst-containing benzoxazine, **NAR-a**, was successfully synthesized using naringenin, aniline, and para-formaldehyde as starting materials. **NAR-a** was shown to readily undergo thermal activation of its latent-catalytic system, the intramolecular hydrogen-bonded -OH, which then efficiently catalyzed the polymerization process without adding any other initiators or catalysts. **NAR-a** was also determined to be an excellent latent polymerization agent for epoxy resins due to the existence of the hydrogen-bonded -OH in the structure. In playing the role of the curing agent, **NAR-a** also acted as an excellent property modifier for epoxy thermosetting systems. The resulting thermoset based on the **NAR-a** modified epoxy resin showed high thermal stability, with a T_g temperature of

201 °C, a T_{d10} temperature of 374 °C, and a low CTE value of 32.4 ppm per °C. Moreover, this thermoset is also a non-ignitable material with HRC of 159.1 J g⁻¹ K⁻¹ and THR of 18.5 kJ g⁻¹. Therefore, the combination of the latent-catalyzed polymerization characteristic and the outstanding thermal properties endow this newly developed benzoxazine/epoxy thermosetting system with extremely promising properties, making it an attractive candidate for high-performance and flame-resistant materials.

Conflicts of interest

There are no conflicts to declare.

Acknowledgements

The authors gratefully acknowledge the partial financial supports of the Natural Science Foundation of China (51603093) and China Postdoctoral Science Foundation (2018T110451).

Notes and references

- 1 R. Auvergne, S. Caillol, G. David, B. Boutevin and J. P. Pascault, *Chem. Rev.*, 2014, **114**, 1082–1115.
- 2 E. M. Petrie, *Epoxy Adhesive Formulations*, McGraw-Hill, New York, 2006.
- 3 S. Wang, S. Ma, C. Xu, Y. Liu, J. Dai, Z. Wang, X. Liu, J. Chen, X. Shen, J. Wei and J. Zhu, *Macromolecules*, 2017, **50**, 1892–1901.
- 4 X. Wang and J. K. Gillham, *J. Appl. Polym. Sci.*, 1991, **43**, 2267–2277.
- 5 Y. Qi, J. Wang, Y. Kou, H. Pang, S. Zhang, N. Li, C. Liu, Z. Weng and X. Jian, *Nat. Commun.*, 2019, **10**, 1–9.
- 6 K. R. Hart, N. R. Sottos and S. R. White, *Polymer*, 2015, **67**, 174–184.
- 7 H. Lee and K. Neville, *Handbook of Epoxy Resins*, McGraw-Hill, New York, 1967.
- 8 I. Hamerton, B. J. Howlin, J. R. Jones, S. Liu and J. M. Barton, *J. Mater. Chem.*, 1996, **6**, 305–310.
- 9 Y. R. Ham, D. H. Lee, S. H. Kim, Y. J. Shin, M. Yang and J. S. Shin, *J. Ind. Eng. Chem.*, 2010, **16**, 728–733.
- 10 K. Kudo, M. Furutani and K. Arimitsu, *ACS Macro Lett.*, 2015, **4**, 1085–1088.
- 11 K. Zhang, X. X. Tan, Y. T. Wang and H. Ishida, *Polymer*, 2019, **168**, 8–15.
- 12 H. Ishida and D. J. Allen, *J. Polym. Sci., Part A: Polym. Chem.*, 1996, **34**, 1019–1030.
- 13 K. Zhang, M. C. Han, L. Han and H. Ishida, *Eur. Polym. J.*, 2019, **116**, 526–533.
- 14 A. F. M. El-Mahdy and S. W. Kuo, *Polym. Chem.*, 2018, **9**, 1815–1826.
- 15 F. Shan, S. Ohashi, A. Erlichman and H. Ishida, *Polymer*, 2018, **157**, 38–49.
- 16 J. Wu, Y. Xi, G. T. Mccandless, Y. Xie, R. Menon, Y. Patel, R. Menon, Y. Patel, D. J. Yang, S. T. Iacono and B. M. Novak, *Macromolecules*, 2015, **48**, 6087–6095.

- 17 K. Zhang, L. Han, P. Froimowicz and H. Ishida, *Macromolecules*, 2017, **50**, 6552–6560.
- 18 C. F. Wang, Y. C. Su, S. W. Kuo, C. F. Huang, Y. C. Sheen and F. C. Chang, *Angew. Chem. Int. Ed.*, 2006, **45**, 2248–2251.
- 19 H. Ishida and T. Agag, *Handbook of Benzoxazine Resins*, Elsevier, Amsterdam, 2011.
- 20 H. Ishida and P. Froimowicz, *Advanced and Emerging Polybenzoxazine Science and Technology*, Elsevier, Amsterdam, 2017.
- 21 X. Ning and H. Ishida, *J. Polym. Sci., Part A: Polym. Chem.*, 1994, **32**, 1121–1129.
- 22 N. N. Ghosh, B. Kiskan and Y. Yagci, *Prog. Polym. Sci.*, 2007, **32**, 1344–1391.
- 23 H. Ishida and D. J. Allen, *Polymer*, 1996, **37**, 4487–4495.
- 24 W. Zhang, P. Froimowicz, C. R. Arza, S. Ohashi, Z. Xin and H. Ishida, *Macromolecules*, 2016, **49**, 7129–7140.
- 25 K. Zhang, Y. Liu, M. Han and P. Froimowicz, *Green Chem.*, 2020, **22**, 1209–1219.
- 26 C. Hsuan Lin, Y. R. Feng, K. H. Dai, H. C. Chang and T. Y. Juang, *J. Polym. Sci., Part A: Polym. Chem.*, 2013, **51**, 2686–2694.
- 27 S. Ohashi, J. Kilbane, T. Heyl and H. Ishida, *Macromolecules*, 2015, **48**, 8412–8417.
- 28 K. Zhang and X. Yu, *Macromolecules*, 2018, **51**, 6524–6533.
- 29 N. K. Sini and T. Endo, *Macromolecules*, 2016, **49**, 8466–8478.
- 30 J. Dunkers and H. Ishida, *Spectrochim. Acta*, 1995, **51**, 1061–1074.
- 31 L. Han, D. Iguchi, P. Gil, T. R. Heyl, V. M. Sedwick, C. R. Arza, S. Ohashi, D. J. Lacks and H. Ishida, *J. Phys. Chem. A*, 2017, **121**, 6269–6282.
- 32 C. H. Lin, Y. S. Shih, M. W. Wang, C. Y. Tseng, T. C. Chen, H. C. Chang and T. Y. Juang, *Polymer*, 2014, **55**, 1666–1673.
- 33 L. Han, M. L. Salum, K. Zhang, P. Froimowicz and H. Ishida, *J. Polym. Sci., Part A: Polym. Chem.*, 2017, **55**, 3434–3445.
- 34 J. A. Dudek and J. A. Kargol, *Int. J. Thermophys.*, 1988, **9**, 245–253.
- 35 I. Hamerton, S. Thompson and B. J. Howlin, *Macromolecules*, 2013, **46**, 7605–7615.
- 36 J. Wang, M. Wu, W. Liu, S. Yang, S. Bai, Q. Ding and Y. Li, *Eur. Polym. J.*, 2010, **46**, 1024–1031.
- 37 D. W. Van Krevelen, *Polymer*, 1975, **16**, 615–620.
- 38 S. Mallakpour and V. Behranvand, *Colloid Polym. Sci.*, 2015, **293**, 333–339.
- 39 R. E. Lyon, N. Safronava, J. G. Quintiere, S. I. Stoliarov, R. N. Walters and S. Crowley, *Fire Mater.*, 2014, **38**, 264–278.
- 40 R. E. Lyon and R. N. Walters, *J. Anal. Appl. Pyrol.*, 2004, **71**, 27–46.
- 41 J. Liu, N. Safronava, R. E. Lyon, J. Maia and H. Ishida, *Macromolecules*, 2018, **51**, 9982–9991.
- 42 K. Zhang, X. Yu and S. W. Kuo, *Polym. Chem.*, 2019, **10**, 2387–2396.